The Thai Journal of Veterinary Medicine

Volume 51
Issue 3 *September, 2021*

Article 16

9-1-2021

UPLC-QTOF/MS-based metabolomic analysis of plasma reveals altitude effects on yaks (Bos grunniens)

Xiangqiong Meng

Juan Zhou

Juan Zhou

Ruidong Wan

Hongxian Yu

See next page for additional authors

UPLC-QTOF/MS-based metabolomic analysis of plasma reveals altitude effects on yaks (Bos grunniens)

Authors

Xiangqiong Meng, Juan Zhou, Juan Zhou, Ruidong Wan, Hongxian Yu, and Qing Wei

Original Article

UPLC-QTOF/MS-based metabolomic analysis of plasma reveals altitude effects on yaks (*Bos grunniens*)

Xiangqiong Meng[1,3] Juan Zhou[2] Jingyi Li[1] Ruidong Wan[2,3] Hongxian Yu[2,3] Qing Wei[1,3*]

Abstract

The yak is an ideal animal model for the study of adaptation to hypoxia at high altitudes. Its blood metabolites are an important reference index for research regarding adaptation to high-altitude hypoxia and can reflect cellular activity, antioxidant capacity and the metabolic capacity of yaks, thus highlighting the adaptability of the yak to hypoxic environments. The aim of our study was to evaluate differences in the global metabolic profiles of plasma in high- and low-altitude yaks (average age: 3 years old; live weight (LW): 300 ± 50 kg) using untargeted metabolomics. 52 differential metabolites were identified; 13 metabolites such as choline and trimethylamine N-oxide showed upregulated expression and 39 different metabolites such as L-carnitine and oleic acid were downregulated. Most of them were involved in energy, lipid and amino acid metabolism pathways. After analysis, the lysosome, citrate cycle, histidine metabolism and fatty acid biosynthesis changed significantly. The results demonstrate that there were differences in the metabolomes of high- and low-altitude yaks. As altitude increases, the critical pathways involve lysosomes, citrate cycle, histidine metabolism, fatty acid biosynthesis and biosynthesis of unsaturated fatty acids.

Keywords: yak, different altitudes, plasma, untargeted metabolomics

[1]*College of Eco-Environmental Engineering, Qinghai University, Xining, Qinghai, China*
[2]*Department of Veterinary Medicine, College of Agriculture and Animal Husbandry, Qinghai University, Xining, Qinghai, China*
[3]*State Key Laboratory of Plateau Ecology and Agriculture, Qinghai University, Xining, Qinghai, China*
***Correspondence**: xwq3519@sina.com* (Q. Wei)
Received February 21, 2021.
Accepted May 11, 2021.
doi: https://doi.org/10.14456/tjvm.2021.66

Introduction

The yak (*Bos grunniens*) is an ancient and primitive species in China. It is a mammal that lives at the highest altitudes of the geographical regions often called the "roof of the world". Although a rare animal resource, yaks can provide meat, milk and plush wool for breeders (Qiu *et al*. 2012) and they represent an important pillar of animal husbandry in alpine grasslands. The yak is also an extremely rare and valuable gene bank, which integrates the products and performance of all categories of livestock and its genetic resources have always garnered attention and importance (Bao *et al*. 2019; Wang *et al*. 2017). Therefore, the yak has been the focus of research concerning plateau animals.

Most studies involving yaks have focused on the origin of species, breed cultivation, milk production, as well as meat nutritional value and quality. The adaptability of the yak to hypoxia has attracted increased interest and has been studied in terms of morphology (Kalita and Bhattacharya 2003), physiology (Ding *et al*. 2014; Wang *et al*. 2018), genomics (Ma *et al*. 2020; Zhang *et al*. 2016), transcriptomics (Lan *et al*. 2018; Ma 2019), proteomics (Babar *et al*. 2019; Zuo *et al*. 2017), and other aspects. However, few investigations have focused on the role of metabolism in hypoxic adaptation. The metabolism of an organism is the final result of the interaction of various factors, including genetic, physiological and environmental ones. Different altitudes may cause changes in a series of metabolites and metabolites are the end products of cellular regulatory processes. Metabolite levels can be regarded as the ultimate response of biological systems to genetic or environmental changes (Fiehn 2002).

Metabolomics is an emerging technological and analytical field in systems biology, following genomics, transcriptomics and proteomics (Gertsman and Barshop 2018). The main goal of metabolomics includes the quantitative study of the multiple dynamic responses of organisms to external stimuli, pathophysiological changes and metabolite levels resulting from gene mutations (Nicholson *et al*. 1999). Metabolomics can maximize qualitative and quantitative metabolites in biological systems and reflect the total metabolite information to the greatest extent. Therefore, metabolomics has a lot of information to further explain the physiological condition of an organism using high-throughput methods to study metabolites in biological samples. Untargeted metabolomics is especially useful when there is no a priori metabolic hypothesis. Liquid chromatography coupled to mass spectrometry (LC-MS) has been the preferred choice for untargeted metabolomics, given the versatility in metabolite coverage and the sensitivity of these instruments.

This study aimed to use an ultra-high-performance liquid chromatography-triple/time-of-flight mass spectrometry (UPLC-QTOF/MS) approach to evaluate differences in the global metabolic profiles of plasma in high- and low-altitude yaks and to further explore the effects of different altitudes on the metabolism and normal survival of the yak. The experimental process is shown in Fig 1. The results may provide a reference for the scientific breeding of yaks and may elucidate the mechanisms by which yaks have physiologically adapted to the metabolic cost of maintaining body function while being exposed to different altitudes.

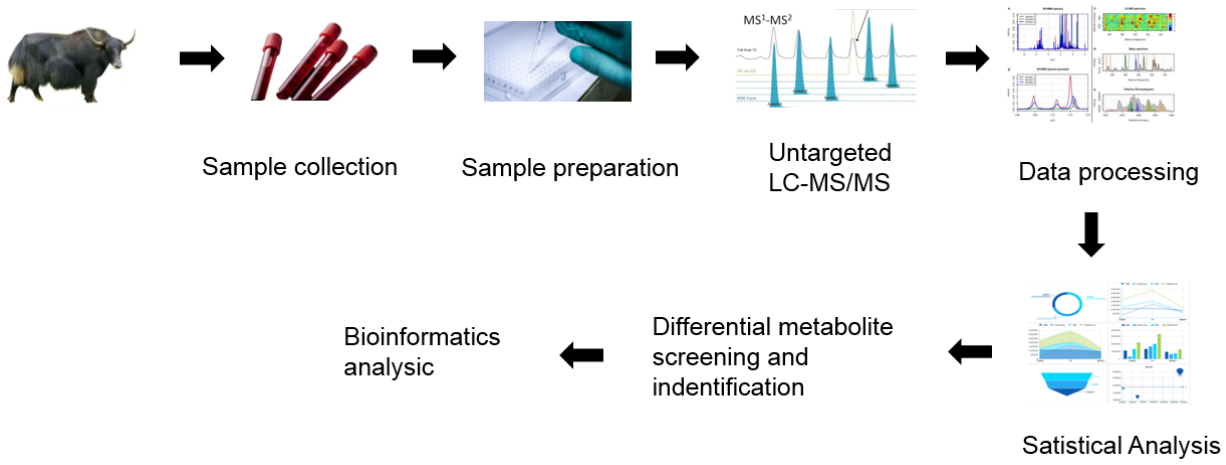

Figure 1 Experimental flowchart.

Materials and Methods

Animals: In total, we studied 12 yaks (6 females and 6 males) about 3 years old from the pastoral area of Qilian County (altitude 4000 m, 100.25° E, 38.18° N) and Xunhua County (altitude 2600 m, 102.49° E, 35.85° N), Qinghai, China. The live weight (LW) of the yaks was about 300 ± 50 kg. Animals from Qilian County represented a high-altitude group, designated as HA. Yaks from Xunhua County comprised a low-altitude cohort termed as LA. The weights and ages of the yaks were similar. This study was approved by the Institutional Animal Care and Use Committee of Qinghai University (Xining, China) and all procedures were performed in accordance with the approved guidelines.

Sample collection: Approximately 4 mL of blood was collected from the neck of the yaks. After collection, the tubes were centrifuged at 1699 × g for 10 mins at 4°C to remove blood cells and plasma was immediately stored at -80°C prior to further processing.

Sample pretreatment: All samples were thawed at 4°C, and 100-µL aliquots were mixed with 400 µL of cold solution (methanol/acetonitrile = 1:1, v/v) to remove proteins. The mixture was centrifuged at 14,000 × g for 20 mins at 4°C. The supernatant was dried in a vacuum centrifuge. For LC-MS analysis, whole samples were treated with an acetonitrile water solution (acetonitrile/water = 1:1 v/v) for testing.

UHPLC analysis: All plasma samples were separated by UHPLC (1290 Infinity LC, Agilent Technologies, USA), equipped with an HILIC column using a 1.7 µm, 2.1 mm × 100 mm ACQUIY UPLC BEH column (Waters, Ireland). In the electrospray ionization (ESI) positive and negative ion modes, the mobile phase contained 25 mM ammonium hydroxide in water, with A = 25 mM ammonium acetate and B = acetonitrile. The elution gradient was 95% B for 0.5 min, which was linearly reduced to 65% over 6.5 mins and then reduced to 40% over 1 min, maintained for 1 min and then returned to 95% in 0.1 min for approximately 3 mins of equilibrium.

Samples were placed in an autosampler at 4°C throughout the analysis. To avoid the influence of instrument detection signal fluctuations, we used a random injection sequence. Regular intervals inserting a Quality control (QC) sample (every 8 samples) throughout the analytical process provided a set of data from which stability and repeatability could be assessed.

Quadrupole-time-of-flight analysis: After UHPLC separation, mass spectrometry analysis was performed with a quadrupole time-of-flight platform (AB Sciex Triple TOF 6600) at Shanghai Applied Protein Technology Co., Ltd. The conditions were as follows: ion source gas 1 (Gas 1) as 40, ion source gas 2 (Gas 2) as 80, curtain gas (CUR) as 30, a source temperature of 650°C and ion spray voltage floating (ISVF) of 5000 V (+) and −5000 V (−). Secondary mass spectrometry data was acquired using information-dependent acquisition (IDA) with the high sensitivity mode selected. The parameters were set as follows: collision energy (CE) fixed at 35 V with ± 15 eV, de-clustering potential (DP) at ± 60 V, excluded isotopes within 4 Da; ten candidate ions were monitored per cycle.

Data analysis: The original data generated by UPLC-Q-TOF/MS was converted to MzXML files with Proteo Wizard MS Convert, before being imported into the XCMS software and filtered through XCMS analysis. For peak selection, the parameters were set as follows: centWave m/z = 25 ppm, peakwidth = c (10, 60), prefilter = c (10, 100) and bw = 5, mzwid = 0.025, minfrac = 0.5 at peak grouping. More than 50% of the variables with non-zero measurement values in at least one group remained in the extracted ion features. Compound identification of metabolites by MS/MS spectra and structural identification of metabolites were performed by mass matching (< 25 ppm) and secondary spectrogram matching, which should be searched and compared using the laboratory database established with available authentic standards. Thereafter, the processed data was uploaded before importing into SIMCA-P14.1 (Umetrics, Umea, Sweden) after normalization of total peak intensity, where it was subjected to multivariate data analysis, including Pareto-scaled principal component analysis (PCA), supervised partial least squares-discriminate analysis (PLS-DA) and orthogonal partial least-squares discriminant analysis (OPLS-DA). Response permutation testing and 7-fold cross-validation were used to evaluate the above-mentioned models. Metabolites with variable importance in the projection (VIP) scores > 1 and $P < 0.05$ were handled with unidimensional statistical analysis using R software, such as the t-test, volcano plot analysis and variation ratio analysis.

For bioinformatics analysis, metabolite relative expression data was used to perform hierarchical clustering analysis. For this purpose, Cluster v.3.0 (http://bonsai.hgc.jp/~mdehoon/software/cluster/software.htm) and Java Treeview software (http://jtreeview.sourceforge.net) were used. The Euclidean distance algorithm for similarity measures and average linkage clustering algorithm (clustering uses the centroids of the observations) for clustering were selected when performing hierarchical clustering. To further explore the impact of differentially expressed metabolites, enrichment analysis was performed. KEGG pathway enrichment analyses were used based on the Fisher's exact test and pathways with P value under a threshold of 0.05 were considered significant. For metabolite annotation and pathway analysis, we performed BLAST searches of the online Kyoto Encyclopedia of Genes and Genomes (KEGG) database (http://geneontology.org/) to retrieve their COs, which were subsequently mapped to pathways in KEGG11 and data on the corresponding KEGG pathways was extracted.

Results

Untargeted metabolomics analysis: A total of 16,756 metabolite ion peaks were extracted from all samples and analyzed by PCA. The distribution of metabolic profiles for the experimental and QC samples in PCA are shown in Fig 2a. QC injections were clustered tightly in the PCA space, indicating that instrument volatility was small and that the experiment was reproducible. Therefore, the experimental data was objective and reliable, the differences in metabolic profiles could describe biological differences and the data could be used for subsequent analysis.

Inter-group PCA analysis: UHPLC-Q-TOF/MS metabolomics profiling for HA and LA produced a total of 9,227 ion peaks under positive modes. After Pareto scaling, PCA indicated differences between HA and LA groups. As shown in Fig 2a, we observed clear separation of HA and LA, which indicated that the spectrum of metabolism in the two groups had changed.

Inter-group PLS-DA and OPLS-DA analysis: First, we screened marker metabolites from comprehensive metabolomics data and established correct discriminant models using PLS-DA. PLS-DA score plots showed a clear distinction between the two

groups (R2Y = 1, Q2 = 0.946; Fig 2b). Thereafter, OPLS-DA was corrected on the basis of PLS-DA to filter out noise that was irrelevant to classification information. The OPLS-DA score plot is shown in Fig 2c (R2Y = 1, Q2 = 0.921). The permutation plot indicated that the original OPLS-DA model was valid and no overfitting was found (R2 = 0.9589, Q2 = −0.09337; Fig 2d). Through these analytical methods, we established a relationship model between metabolite expression levels and the sample category and realized the prediction of the sample category, thereby assisting the screening of marker metabolites.

Univariate statistical analysis: Volcano plot analysis results are shown in Fig 3, illustrating the significance of metabolite changes between the two samples. Red points represent differential metabolites with FC > 1.5 and P < 0.05, which can help in screening potential marker metabolites.

Metabolites with significant differences between groups: A total of 25 differential metabolites (ESI (+)) were identified between the HA and LA groups based on the criteria of VIP > 1 and according to the OPLS-DA model and univariate statistical analysis (Table 1). Among them, twenty-three metabolites were significantly different metabolites (VIP > 1 and P < 0.05) and the remaining two were differential metabolites (VIP > 1 and 0.05 < P < 0.1).

Bioinformatics analysis: To display relationships comprehensively and intuitively between samples and expression patterns of metabolites in different samples, we performed hierarchical clustering for each group of samples. Metabolites gathered in the same cluster showed similar expression patterns. A heatmap of the Spearman rank-order correlation coefficient after hierarchical cluster analysis indicated that metabolite abundances were different in the HA and LA groups (Fig 4). Although some metabolites also showed similarities, significantly different metabolites were identified which could distinguish the two groups.

Significantly different metabolite correlation analysis results are shown in Fig 5a. The metabolites shown in the Figure are all significantly related metabolites (P < 0.05), where blue represents a negative correlation and red represents a positive correlation. The size of the circle is the P value and the depth of the color represents the magnitude of the correlation. A positive correlation implies that the expression trends of the two are the same or similar in function and category, while a negative correlation implies the opposite.

KEGG metabolic pathway analysis of differential metabolites: We analyzed and calculated the significance level of metabolite enrichment of each pathway using the Fisher's exact test to determine signal transduction pathways and metabolic pathways with significant changes. Fig 5b presents KEGG pathway enrichment analysis results of the differentially expressed metabolites in the HA vs. LA groups. The results show that histidine metabolism, TCA cycle, fatty acid biosynthesis, glycine, serine and threonine metabolism, biosynthesis of unsaturated fatty acids and glyoxylate and dicarboxylate metabolism had undergone significant changes.

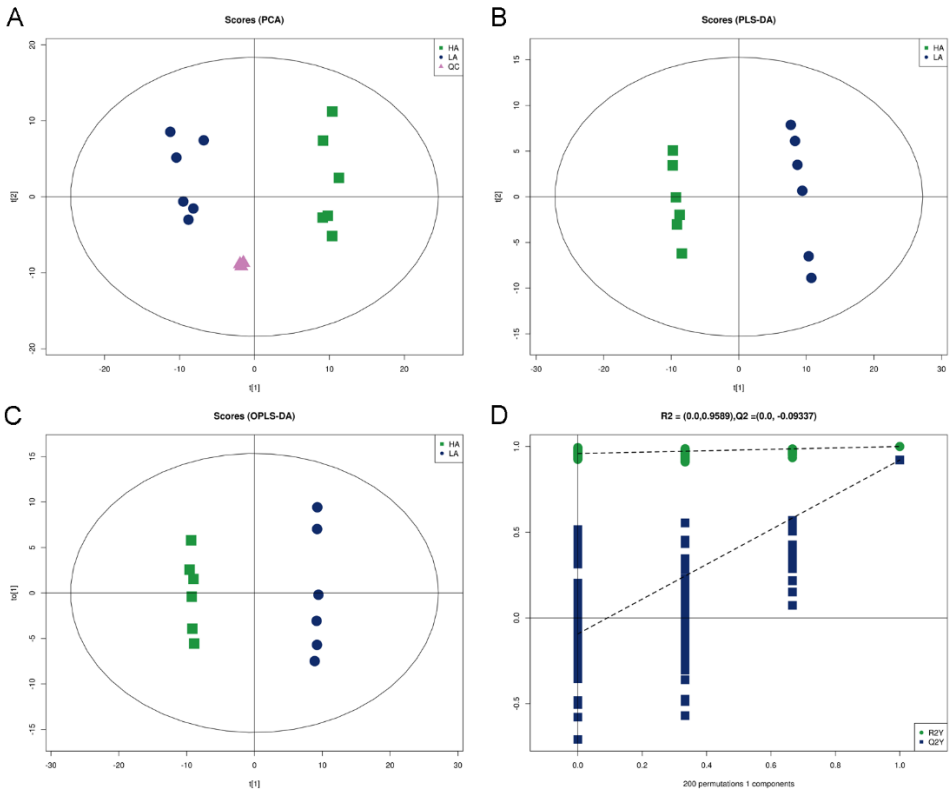

Figure 2 Metabolomic analysis of all samples from LA and HA groups. The PCA model (a), PLS-DA model (b), and OPLS-DA model (c) showed differences between LA and HA groups, respectively. The permutation plot was used to monitor the stable and reliable OPLS-DA model (d).

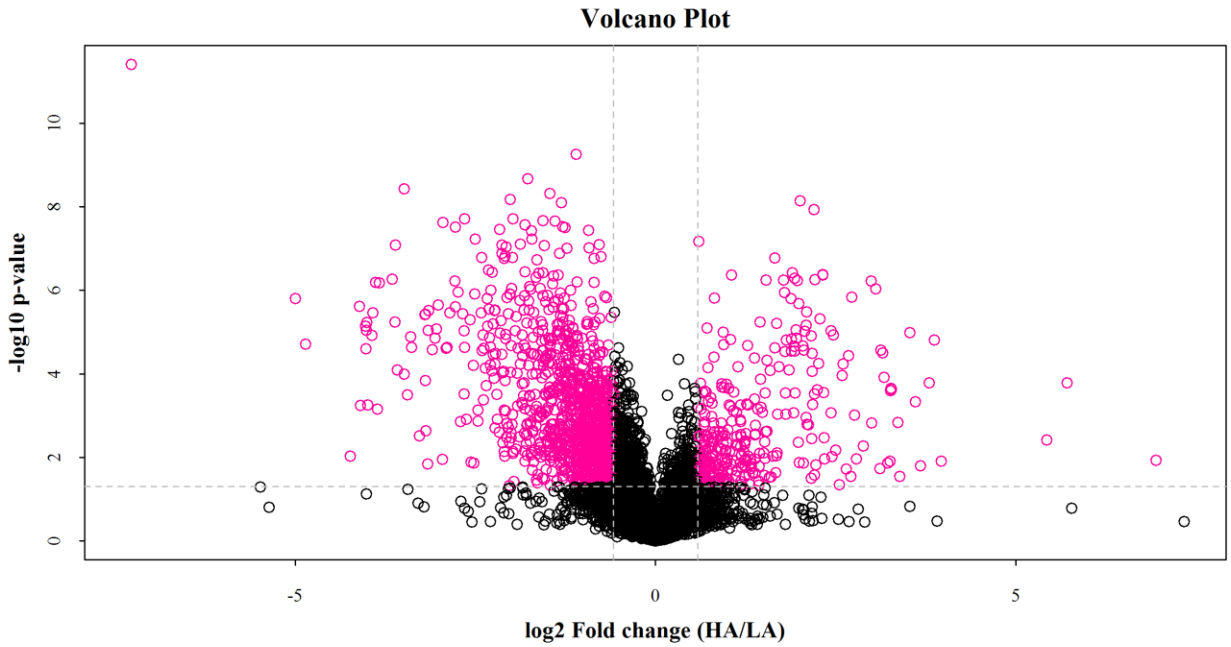

Figure 3 Volcano Plot analysis of differential metabolites.

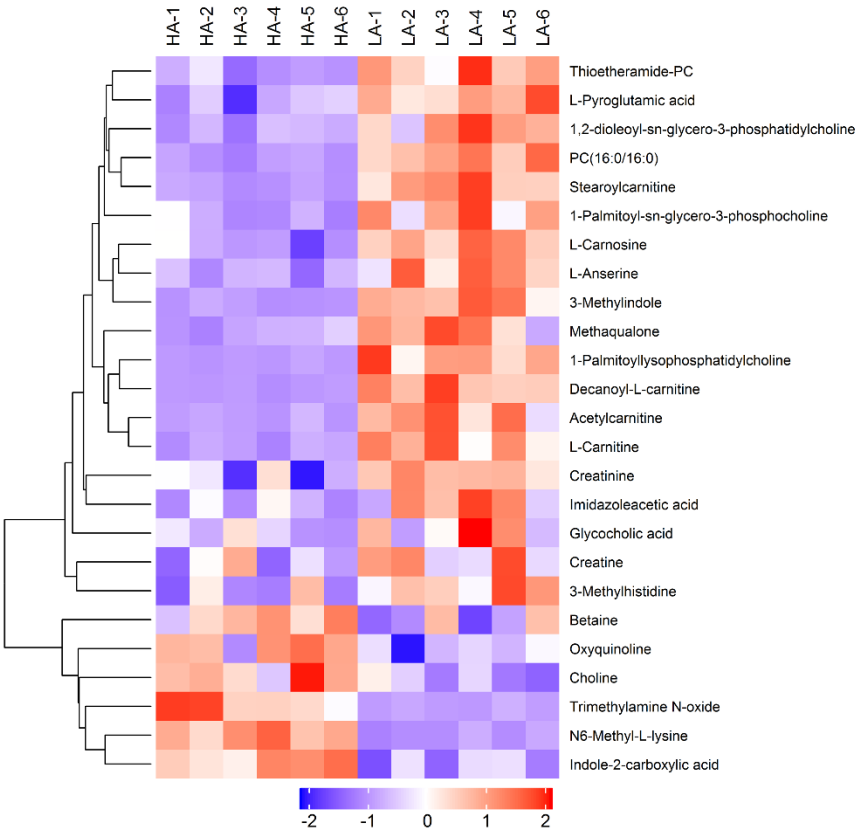

Figure 4 Heatmap of the Spearman rank-order correlation analysis.

Table 1 Differential metabolites identified between the HA and LA groups

Ionization mode	Metabolite	VIP	Fold change	*P*-value	m/z	Rt(s)	Accession no
ESI (+)	L-Carnitine	20.894	0.478	0.000108	162.112	348.051	M161T526
ESI (+)	PC(16:0/16:0)	16.294	0.282	0.000003	756.555	146.034	M162T348_2
ESI (+)	Acetylcarnitine	12.876	0.347	0.000327	204.123	301.477	M757T146_1
ESI (+)	Choline	7.857	1.824	0.005626	104.107	265.294	M204T301
ESI (+)	1-Palmitoyl-sn-glycero-3-phosphocholine	7.295	0.665	0.001947	496.340	193.418	M104T265_2
ESI (+)	Trimethylamine N-oxide	6.978	12.187	0.000461	76.075	326.337	M496T193_2
ESI (+)	Betaine	6.280	1.986	0.044115	118.086	455.203	M76T326
ESI (+)	Thioetheramide-PC	6.062	0.553	0.000292	780.553	143.479	M118T455
ESI (+)	Creatinine	5.207	0.830	0.005673	114.066	167.058	M781T143_1
ESI (+)	3-Methylindole	3.371	0.095	0.000013	132.080	36.717	M114T167_2
ESI (+)	1,2-dioleoyl-sn-glycero-3-phosphatidylcholine	2.869	0.595	0.000940	768.588	140.680	M132T37
ESI (+)	N6-Methyl-L-lysine	2.309	3.459	0.000001	161.128	526.249	M769T141
ESI (+)	1-Palmitoyllysophosphatidylcholine	2.263	0.209	0.000034	538.385	188.251	M538T188
ESI (+)	Oxyquinoline	2.043	1.314	0.014874	146.059	48.778	M146T49
ESI (+)	Imidazoleacetic acid	1.620	0.731	0.023352	144.076	373.927	M144T374
ESI (+)	Glycocholic acid	1.618	0.454	0.099737	466.315	249.264	M466T249
ESI (+)	Creatine	1.577	0.715	0.093216	132.076	339.846	M132T340
ESI (+)	L-Carnosine	1.548	0.687	0.000152	227.113	415.126	M227T415
ESI (+)	3-Methylhistidine	1.458	0.744	0.017674	170.092	378.842	M170T379
ESI (+)	Stearoylcarnitine	1.341	0.192	0.000025	428.372	170.293	M428T170
ESI (+)	L-Anserine	1.311	0.665	0.000889	241.129	410.626	M241T411
ESI (+)	Indole-2-carboxylic acid	1.266	2.758	0.000636	162.054	43.026	M162T43
ESI (+)	Methaqualone	1.221	0.381	0.002281	518.254	36.717	M518T37
ESI (+)	Decanoyl-L-carnitine	1.177	0.121	0.000008	316.248	190.189	M316T190
ESI (+)	L-Pyroglutamic acid	1.155	0.768	0.000315	147.076	368.572	M147T369
ESI (−)	15-keto-PGE1	5.910	4.875	0.002372	333.206	122.194	M333T122
ESI (−)	Tricosanoic acid	1.021	0.421	0.005427	353.341	39.919	M353T40
ESI (−)	Heptadecanoic acid	6.027	0.410	0.006588	269.249	41.552	M269T42
ESI (−)	3-Hydroxydodecanoic acid	1.204	0.269	0.007140	237.149	51.664	M237T52
ESI (−)	Indoxyl sulfate	2.567	2.359	0.015048	212.002	33.597	M212T34_1
ESI (−)	Myristic acid	2.333	1.227	0.015643	227.201	71.495	M227T71
ESI (−)	Arachidic acid	5.753	0.181	0.020543	311.295	39.513	M311T40
ESI (−)	Deoxycholic acid	1.379	0.173	0.021954	391.282	127.908	M391T128
ESI (−)	Taurolithocholic acid	1.353	2.008	0.029494	482.293	74.090	M482T74
ESI (−)	3,3-Dimethylglutaric acid	3.492	0.083	0.029527	159.066	76.021	M159T76
ESI (−)	Citrate	1.267	0.505	0.030858	191.019	531.020	M191T531
ESI (−)	Azelaic acid	1.066	0.255	0.045060	187.097	340.791	M187T341
ESI (−)	D-Ribose	2.970	1.611	0.047553	149.045	88.000	M149T88
ESI (−)	Glycocholic acid	1.292	0.508	0.048455	464.300	249.306	M464T249
ESI (−)	DL-lactate	7.853	0.328	0.050527	89.025	225.304	M89T225
ESI (−)	D-Fructose	1.510	0.510	0.053876	359.119	302.676	M359T303
ESI (−)	cis-9-Palmitoleic acid	7.273	0.264	0.056103	253.217	42.972	M253T43
ESI (−)	2-Oxoadipic acid	1.094	0.899	0.069544	181.009	345.477	M181T345
ESI (−)	Stearic acid	2.292	0.108	0.070531	343.284	32.587	M343T33
ESI (−)	Pentadecanoic Acid	6.219	0.285	0.075203	241.217	44.372	M241T44
ESI (−)	Oleic acid	16.874	0.395	0.075404	281.249	41.552	M281T42
ESI (−)	D-Mannose	2.072	0.376	0.080779	239.077	303.095	M239T303
ESI (−)	all cis-(6,9,12)-Linolenic acid	6.471	0.219	0.082966	277.217	42.262	M277T42
ESI (−)	L-Gulonic gamma-lactone	1.029	1.389	0.086900	237.061	89.228	M237T89
ESI (−)	(+-)5,6-DHET	1.201	0.376	0.090634	337.237	125.195	M337T125
ESI (−)	cis-Aconitate	1.636	1.331	0.091058	173.009	492.876	M173T493
ESI (−)	Mesaconic acid	1.207	0.430	0.098243	129.019	432.519	M129T433

Abbreviations: m/z, mass-to-charge ratio; Rt, retention time; VIP, variance importance for projection; FC, fold change.

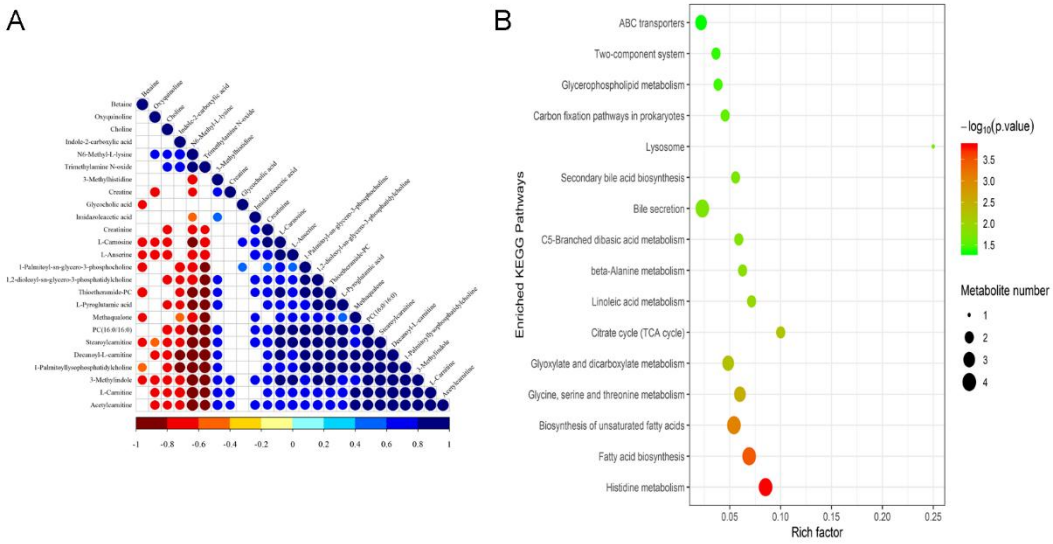

Figure 5 Bioinformatics analysis of differential metabolites. a. Relevance among significant differential metabolites; b. KEGG pathway enrichment analysis of differentially expressed metabolites.

Discussion

The yak is an ideal animal model for the study of adaptation to hypoxia at high altitudes (Ding *et al*. 2014). Metabolites in blood can be used as important reference indicators in the study of adaptation to hypoxia. The changes in measured values of relevant indicators can reflect cell activity, antioxidant capacity and the metabolic capacity of the yak, thus reflecting the adaptability of yaks to hypoxic environments (Podoinitsyna and Kozub 2019). However, the specific factors related to the metabolic cycles in the blood of yaks remain relatively unexplored. To our knowledge, this is the first study that characterized the plasma metabolomes of yaks living at different altitudes using an untargeted approach coupled with UHPLC-Q-TOF MS.

Alterations of several metabolites were observed in the blood of yaks at different altitudes of 2600 m and 4000 m on the Qinghai Plateau. In total, 52 different metabolites (ESI (+) and ESI (−) modes) associated with altitude were identified (Table 1). These metabolites were involved in the TCA cycle, histidine metabolism, fatty acid biosynthesis, glycine, serine and threonine metabolism, biosynthesis of unsaturated fatty acids and glyoxylate and dicarboxylate metabolism.

It is important to note that among all the molecules characterized, two, namely L-carnitine and Phosphatidylcholine (PC) (16:0/16:0), are recognized for their roles in metabolism. Based on the literature, the term hypoxia tends to be used to refer to the partial pressure of atmospheric oxygen, which reduces with increasing altitude. Signals from hypoxia and the resulting hypoxemia prompt the body to produce erythrocytes, which can increase the viscosity of blood and augment pulmonary arterial pressure. More recent evidence suggests that NO is a potent vasodilator and its production has been implicated in the pathogenesis of pulmonary hypertension (Ma *et al*. 2019). L-carnitine, a natural compound, exerts antioxidant effects and decreases lipid peroxidation. Carnitine can transport long-chain fatty acids, which are converted into biological energy across inner mitochondrial membranes by alpha-oxidation (Martínez *et al*. 2004). Therefore, L-carnitine plays a critical role in oxidation to provide cellular energy. Erbas and Sharifi (Erbas *et al*. 2007; Sharifi *et al*. 2009) *et al*., indicated that L-carnitine increased NO abundance by reducing the activity of arginase and angiotensin-converting enzyme in the aorta, heart and kidneys or by elevating NO synthase activity, resulting in higher NO production. Thus, L-carnitine can be beneficial in attenuating the oxidative stress associated with high altitudes and it demonstrates a beneficial effect in improving the cardiopulmonary function of yaks. In this study, PC (16:0/16:0) had higher VIP values, which indicated that PC (16:0/16:0) played a critical role in hypoxic adaptation and its expression level decreased with increasing altitude. PC (16:0/16:0) is a subclass of glycerophospholipids and its biological functions include membrane stability, cell signaling, fuel and energy source/storage, as well as roles in phospholipid metabolism (Chen *et al*. 2017). The higher the saturation of phospholipids, the stronger the interaction of fatty acids and the poorer the membrane fluidity, which increases the risk of atherosclerotic plaque. PC (16:0/16:0) is a saturated phospholipid and a reduction in its expression is the yak's adaptation strategy to high-altitude and low-oxygen environments. Studies suggest that PC may be recognized as a potential indicator for the prediction of the risk of vascular disease.

In general, 52 different metabolites are involved in amino acid metabolism, energy metabolism and lipid metabolism. Certain changes have occurred at different altitudes and their high VIP levels suggest the importance of these pathways in adaptation to hypoxia. It is known that mammals can utilize glycolysis, the TCA cycle and oxidative phosphorylation to generate energy from glucose. The TCA cycle is one of the hallmark pathways in energy metabolism. It is well known that this process is responsible for the oxidation of respiratory substrates to drive ATP synthesis. During hypoxia, the lack of oxygen delivery results in decreased levels of ATP, increased accumulation of lactate and alterations of

several metabolites (Cao *et al*. 2017). Jansen Seheult and colleagues have also shown that an inadequate oxygen supply slows TCA cycle-associated metabolism and leads to increased production of lactate from pyruvate (Seheult *et al*. 2017). In order to meet energy requirements under hypoxic conditions, glycolysis is enhanced, whereas the accumulation of considerable amounts of lactic acid has the potential to disrupt and damage normal physiological functions (Feenstra *et al*. 2014). This shows that in a high-altitude environment, the body generates energy by enhancing glycolysis to adapt to a low-oxygen environment. Inhibition of the TCA cycle and an increase in glycolysis metabolism under hypoxic conditions are the result of the coordinated regulation of hypoxia involving the two production pathways. In the present study, the content of lactic acid in plasma decreased with increased altitude, indicating that yaks could adapt well to high-altitude and low-oxygen environments (http://www.kegg.jp/kegg-bin/show_pathway?map00020+C00158+C00417). However, we currently have no evidence to explain the mechanisms of adaptation to lactate under hypoxic conditions.

We found that among the lipid metabolism pathways, those most affected by different altitudes involved unsaturated fatty acids and the biosynthesis of fatty acids (http://www.kegg.jp/kegg-bin/show_pathway?map01040+C06425+C01530+C00712+C06426; http://www.kegg.jp/kegg-bin/show_pathway?map00061+C06424+C08362+C01530+C00712). This leads to a decrease in circulating free fatty acids, such as stearic acid, arachidic acid, oleic acid and cis-9-palmitoleic acid between the LA and HA groups, which exhibited fold changes > 2.53, indicating that lipid metabolism decreased with increasing altitude. The effect of hypoxic status on lipid metabolism is controversial and some studies suggest hypoxia as an increase or decrease in cytoplasmic lipid metabolism (Lin *et al*. 2006; Park *et al*. 2010). Additionally, another report demonstrated that the target genes of the HIF pathway that were sensitive to hypoxia could regulate lipid metabolism by activating insulin sensitivity or HIF-1α could suppress fatty acid β-oxidation (Krishnan *et al*. 2012). It has been described that hypoxia inhibits adipogenesis by reducing PPARγ2 expression (Lin *et al*. 2009; Sang *et al*. 2010). Our results are similar to those of other studies that have shown that hypoxia inhibits lipid metabolism by decreasing the expression of fatty acid metabolites, including stearic acid, arachidonic acid and oleic acid.

In amino acid metabolism, five different metabolites are enriched in histidine metabolism and glycine, serine and threonine metabolism (http://www.kegg.jp/kegg-bin/show_pathway?map00340+C00386+C01262+C01152+C02835; http://www.kegg.jp/kegg-bin/show_pathway?map00260+C00114+C00719+C00300). Studies have shown that under hypoxic conditions, differentially expressed genes are significantly enriched in metabolic pathways involving glycine, serine and threonine (Xiao *et al*. 2017). Moreover, organisms can modulate the activation of oxidoreductases in glycine, serine and threonine metabolism pathways to adapt to hypoxic environments (Zhigalova *et al*. 2015).

In the present study, the lysosomal pathway exhibited the highest rich factor value, which implies that lysosomal metabolic pathways were most affected by altitude changes (http://www.kegg.jp/kegg-bin/show_pathway?map04142+C00159). We suggest that the yak relies on a lysosome-based autophagy process to remove harmful metabolites, such as excess lactic acid and fat, arising due to hypoxia to avoid cell acidosis and cardiovascular diseases such as atherosclerosis caused by fat accumulation, in order to adapt to high-altitude areas and low-oxygen environments. The lysosomal pathway is a universal catabolic process that interacts with other organelles through special membrane regions involving related organelles to achieve the transmission of metabolites and signaling molecules. Autophagy is a highly conserved process that can degrade most cytoplasmic components (Li *et al*. 2020). Additionally, autophagy is a process through which the body regulates cell metabolism and self-protection mechanisms to counter pathophysiological reactions such as injury, stress and hypoxia (Zhou *et al*. 2016). Under pathophysiological conditions, cells can remove proteins and necrotic organelles and destroy cells through autophagy, thereby maintaining homeostasis of cells and organisms (Carini *et al*. 2004; Zhou *et al*. 2016).

In conclusion, this work demonstrated the identification of metabolic pathways in the plasma of yaks associated with adaptation to hypoxia at high altitudes using UHPLC-Q-TOF/MS-based metabolomics. The results show that differences in altitude exhibit the most remarkable impact on lysosomes, energy metabolism, amino acid metabolism and fat synthesis. Yaks can better adapt to hypoxic environments by modulating metabolic pathways and interactions between various metabolic pathways.

Acknowledgements

We are grateful to Qinwen Zhang and Haixia Jing for their assistance in sample collection.

References

Babar A, TD Mipam, S Wu, *et al*. 2019. Comparative iTRAQ Proteomics Identified Myocardium Proteins Associated with Hypoxia of Yak. Current Proteomics. 16:314-329.

Bao P, J Pei, X Ding, *et al*. 2019. Characterisation of the complete mitochondrial genome of the Jinchuan Yak (Bos grunniens). Mitochondrial DNA Part B-Resources. 4:3856-3857.

Cao XF, ZZ Bai, L Ma, *et al*. 2017. Metabolic Alterations of Qinghai-Tibet Plateau Pikas in Adaptation to High Altitude. High Alt Med Biol. 18:219-225.

Carini R, R Castino, MG De Cesaris, *et al*. 2004. Preconditioning-induced cytoprotection in hepatocytes requires Ca2+-dependent exocytosis of lysosomes. Journal of Cell Science. 117:1065-1077.

Chen Y, S Wen, M Jiang, *et al*. 2017. Atherosclerotic dyslipidemia revealed by plasma lipidomics on ApoE/ mice fed a high-fat diet. Atherosclerosis. 262:78-86.

Ding XZ, CN Liang, X Guo, *et al*. 2014. Physiological insight into the high-altitude adaptations in

domesticated yaks (Bos grunniens) along the Qinghai-Tibetan Plateau altitudinal gradient. Livestock Science. 162:233-239.

Erbas H, N Aydogdu, U Usta, *et al*. 2007. Protective role of carnitine in breast cancer via decreasing arginase activity and increasing nitric oxide. Cell Biology International. 31:1414-1419.

Feenstra RA, MKP Kiewiet, EC Boerma, *et al*. 2014. Lactic acidosis in diabetic ketoacidosis. BMJ Case Reports. 2014:bcr2014203594.

Fiehn OJPMB. 2002. Metabolomics – the link between genotypes and phenotypes. Plant Molecular Biology. 48:155-171.

Gertsman I, and BA Barshop. 2018. Promises and pitfalls of untargeted metabolomics. J Inherit Metab Dis. 41:355-366.

Kalita HC, and R Bhattacharya. 2003. Comparative morphology of the alveolar cells in the lung of mithun (Bos frontalis), yak (Bos grunniens) and zebu (Bos indicus). Indian Journal of Animal Sciences. 73:1202-1203.

Krishnan J, C Danzer, T Simka, *et al*. 2012. Dietary obesity-associated Hif1α activation in adipocytes restricts fatty acid oxidation and energy expenditure via suppression of the Sirt2-NAD+ system. Genes Dev. 26:259-270.

Lan, DaoLiang, Xiong, *et al*. 2018. Transcriptome profile and unique genetic evolution of positively selected genes in yak lungs. GENETICA – DORDRECHT. 146:151-160.

Li J, G Liu, L Li, *et al*. 2020. Research progress on the effect of autophagy-lysosomal pathway on tumor drug resistance. Experimental Cell Research. 389:111925.

Lin Q, Z Gao, RM Alarcon, *et al*. 2009. A role of miR-27 in the regulation of adipogenesis. FEBS J2. 76:2348-2358.

Lin Q, YJ Lee, and ZJJoBC Yun. 2006. Differentiation Arrest by Hypoxia. Journal of Biological Chemistry. 281:30678-30683.

Ma J, L Chen, J Fan, *et al*. 2019. Dual-targeting Rutaecarpine-NO donor hybrids as novel anti-hypertensive agents by promoting release of CGRP. European Journal of Medicinal Chemistry. 168:146-153.

Ma X, D Fu, M Chu, *et al*. 2020. Genome-Wide Analysis Reveals Changes in Polled Yak Long Non-coding RNAs in Skeletal Muscle Development. Frontiers in Genetics. 11:365.

Martínez L, A Sánchez-Escalante, JA Beltrán, *et al*. 2004. Antioxidant effect of carnosine and carnitine in fresh beef steaks stored under modified atmosphere. Food Chemistry. 85:453-459.

Nicholson JK, JC Lindon, and EJX Holmes. 1999. \"Metabonomics\": understanding the metabolic responses of living systems to pathophysiological stimuli via multivariate statistical analysis of biological NMR spectroscopic data. Xenobiotica. 29:1181-1189.

Park YS, Y Huang, YJ Park, *et al*. 2010. Specific down regulation of 3T3-L1 adipocyte differentiation by cell-permeable antisense HIF1α-oligonucleotide. Journal of Controlled Release. 144:82-90.

Podoinitsyna TA, and YA Kozub. 2019. Regular changes in hematological and biochemical indicators and immunogenetic certification of yak blood introduced in new conditions. IOP Conference Series: Earth and Environmental Science. 315:042007(5 pp).

Qiu Q, G Zhang, T Ma, *et al*. 2012. The yak genome and adaptation to life at high altitude. Nature Genetics. 44:946-949.

Sang YK, AY Kim, HW Lee, *et al*. 2010. miR-27a is a negative regulator of adipocyte differentiation via suppressing PPARgamma expression. Biochemical & Biophysical Research Communications. 392:323-328.

Seheult J, G Fitzpatrick, and G Boran. 2017. Lactic acidosis: an update. Clinical Chemistry and Laboratory Medicine. Clin Chem Lab Med. 55:322-333.

Sharifi A, B Zare, M Keshavarz, *et al*. 2009. Effect of short term treatment of L-carnitine on tissue ACE activity in streptozotocin-induced diabetic rats. Pathophysiology. 16:53-56.

Wang Q, QW Zhang, Y Zhang, *et al*. 2018. Analysis of production traits,physiological and biochemical index of yak.

Wang Y, J Zhu, H Cai, *et al*. 2017. Crucial genes at the onset of lactation revealed by transcriptome screening of domestic yak mammary gland. Canadian Journal of Animal Science. 97:448-455.

Xiao B, L Li, C Xu, *et al*. 2017. Transcriptome sequencing of the naked mole rat (Heterocephalus glaber) and identification of hypoxia tolerance genes. Biology Open. 6:1904-1912.

Zhang X, K Wang, L Wang, *et al*. 2016. Genome-wide patterns of copy number variation in the Chinese yak genome. Bmc Genomics. 17:379.

Zhigalova N, A Artemov, A Mazur, *et al*. 2015. Transcriptome sequencing revealed differences in the response of renal cancer cells to hypoxia and CoCl 2 treatment. F1000Research. 4:1518.

Zhou J, W Shi, L-H Li, *et al*. 2016. A Lysosome-Targeting Fluorescence Off-On Probe for Imaging of Nitroreductase and Hypoxia in Live Cells. Chemistry-an Asian Journal. 11:2719-2724.

Zuo H, L Han, Q Yu, *et al*. 2017. Proteomics and Bioinformatics Analyses of Differentially Expressed Proteins in Yak and Beef Cattle Muscle. Transactions of the Chinese Society for Agricultural Machinery. 48:313-320.